Accepted Manuscript

Activation energy and binary chemical reaction effects in mixed convective nanofluid flow with convective boundary conditions

Mlamuli Dhlamini, Peri K. Kameswaran, Precious Sibanda, Sandile Motsa, Hiranmoy Mondal

Please cite this article as: M. Dhlamini, P.K. Kameswaran, P. Sibanda, S. Motsa, H. Mondal, Activation energy and binary chemical reaction effects in mixed convective nanofluid flow with convective boundary conditions, *Journal of Computational Design and Engineering* (2018), doi: https://doi.org/10.1016/j.jcde.2018.07.002

Activation energy and binary chemical reaction effects in mixed convective nanofluid flow with convective boundary conditions

Mlamuli Dhlamini[a], Peri K. Kameswaran[b], Precious Sibanda[a], Sandile Motsa[a,c], Hiranmoy Mondal[a]

[a]School of Mathematics, Statistics and Computer Science,University of KwaZulu-Natal, Private Bag X01, Scottsvile, Pietermaritzburg-3209, South Africa

[b]Department of Mathematics, School of Advanced Sciences, VIT University, Vellore 632014, India

[c]Department of Mathematics, University of Swaziland, Private Bag 4, Kwaluseni, Swaziland

Abstract

In this paper we present a theoretical study of the combined effects of activation energy and binary chemical reaction in an unsteady mixed convective flow over a boundary of infinite length. The current study incorporates the influence of the Brownian motion, thermophoresis and viscous dissipation on the velocity of the fluid, temperature of the fluid and concentration of chemical species. The equations are solved numerically to a high degree of accuracy using the spectral quasilinearisation method. Brownian motion was noted as the main process by which the mass is transported out of the boundary layer. The effect of thermophoretic parameter seems to be contrary to the expected norm. We expect the thermophoretic force to 'push' the mass away from the surface thereby reducing the concentration in the boundary layer, however concentartion of chemical species is seen to increase in the boundary layer with an increase in the the thermophoretic parameter. The use of a heated plate of infinite length increased the concentration of chemical species in the boundary layer. The Biot number which increases and exceeds a value of one for large heated solids immersed in fluids increases the concentration of chemical species for its increasing values.

Keywords: Arrhenius Activation energy, Binary chemical reaction, Viscous dissipation,

*Corresponding author
Email address:* hiranmoymondal@yahoo.co.in (Hiranmoy Mondal)

Brownian motion, Thermophoresis

1. Introduction

The study of boundary layer flow of a mixture of fluids with heat and mass transfer past a continuous surface has a lot of applications in aerodynamics, extrusion of plastic and rubber sheets, crystal growing and so on [1, 2]. The Arrhenius activation term was introduced in 1889 by Svante Arrhenius. It models the minimum energy which must be available to a chemical system with potential reactants to produce a chemical reaction. Filippos *et al.* [3] suggested that in a successful reaction, it is reasonable to assume that a reaction occurs with a certain nonzero probability. In the study, the researchers investigated the effect of varying this probability on the rate of reaction. A binary chemical reaction is a reaction that occurs in two steps. These types of reaction are common in deposition processes, both chemical vapour deposition (CVD) and chemical liquid deposition (CLD). Chemical deposition has industrial applications such as coating of metallic objects and glasses, manufacture of electronic devices eg diodes and transistors, gas-permeation barriers and many other applications [4]. In a binary chemical reaction, the activation energy has been shown to be a significant factor [2]. During a chemical deposition process the reaction must occur on the surface of the substrate [4]. Since the reactor chamber is heated from outside, some reactions may occur away from the substrate surface leading to a processes known as the gas phase nucleation and this presents a major problem [5]. In order to ensure that atomic layer deposition (ALD) surface reactions take place and not the CVD-like reactions, one can execute a purge step after each half-cycle to remove the residual precursor or reactants [6]. Despite not being understood fully, the liquid phase deposition (LPD) or chemical liquid deposition is superior to other deposition techniques because of low processing temperature, simplicity of the equipment, high growth rate ($12nm/h$) and low operational cost [7]. In order to improve/enhance thermal properties of fluid for industrial applications ordinary fluids are normally replaced with nanofluids. The term nanofluid was coined by Choi in 1995 [8] to describe fluids where nano-sized particles are added. The material used range from stable

2

metals, oxides, carbides, nitrates and non-metals [9, 10, 11, 12]. In this study we focus on the flow of a binary chemically reacting fluid with Arrhenius activation energy and convective boundary conditions. This study seeks to address the impact that activation energy and frictional heating among other factors have on the flow of such fluids. An understanding of the influence of frictional heating on a binary chemical reaction may help in the elimination of premature reactions occurring away from the surface of the substrate and thus improve the deposition. Heat transport in stretching or moving sheets and ambient fluid has become very critical in most engineering applications [13]. In this study we consider the concentration of one of the end products of the chemical reaction rather than tracking the concentration of the reactants. The study of the combined effects of activation energy and binary chemical reactions have been considered by several researcher [14, 15, 16, 17, 18, 19]

Makinde and Olanrewaju's [1] study focused on the buoyancy parameter, i.e. thermal and solutal Grashof number. They showed that the momentum boundary layer thickness generally decreased with increasing buoyancy parameter values. Reverse flow within the boundary layer was shown to occur with increasing buoyancy values. Wall suction causes the momentum boundary layer to decrease while injection causes the momentum boundary layer to increase. An increase in the Damkohler parameter was shown to increase the temperature of the fluid. An increase in the Damkohler parameter reduced the concentration of chemical species in the boundary layer. The Schmidt number was however shown to have a reverse effect on the boundary layer. An increase in the Schmidt number causesd the species concentration to increase within the boundary layer. Results from [15] show that a reverse flow within the boundary layer is enhanced with an increase in the intensity of buoyancy forces, injection, destructive chemical reaction, radiation absorption, and thermo-diffusion effect and a decrease in the diffusion-thermal effect and also that fluid temperature increases. The species concentration decreases with an increase in Soret number and a decrease in Dufour number. Abbas *et al.* [16] conclude that increasing values of non-dimensional activation energy enhances the concentration profile within the boundary layer. Maleque [17] found that a small decrease in temperature profile is found for increasing values of the preexposure

3

parameter for exothermic reaction, but opposite effects are found for endothermic reaction. The chemical reaction rate decreases with increasing activation energy. He further concluded that the velocity and temperature profiles increase with increasing chemical reaction rate constant for exothermic reaction, but opposite effects are found for endothermic reaction. Buoyancy and heat generation/absorption were shown to have marked effects on the boundary layer and velocity profile in [18]. The effect of heat generation coefficient is to expand the boundary layer thickness and opposite effect is found for heat absorption. Thus, the heat generation/absorption coefficient has the same effects on skin-friction coefficients. The effect of rotation was studied by Awad *et al.* [20]. He showed that for small values of the rotation rate parameter a monotonic exponential decay in the velocity profiles was observed and an oscillatory decay for large values.

The objective of this study is to investigate the unsteady flow with activation energy and binary chemical reaction over a boundary of infinite length. The temperature condition at the boundary depends on the Biot number. The model equations are solved numerically using a recently developed spectral quasi-linearization method. The second objective is to explore the accuracy and convergence of the method through the evaluation of the residual errors norms, and to investigate the impact of flow parameters on the transport processes. The results may give insights as to the choice of parameter values that may be used in engineering applications. The influence of pertinent parameters on the physical quantities has been examined graphically.

2. Mathematical Analysis

Consider the flow of an unsteady one dimensional viscous nanofluid over an infinitely long flat plate moving with velocity U_0 in a binary chemical mixture. Since the plate is infinite and the motion is unsteady all the flow variables depend only on y and time t. The temperature and concentration far from the wall are T_∞ and C_∞.
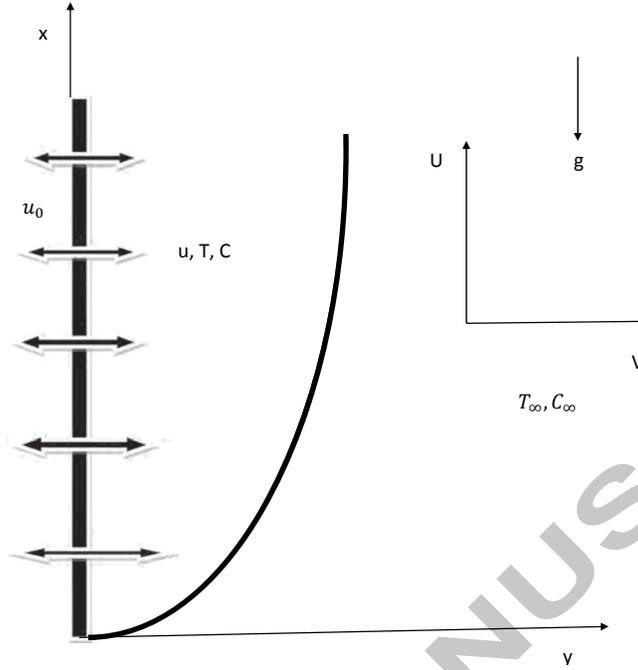
4

Figure 1: Flow configuration and coordinate system

The geometry of the problem is chosen in the Cartesian coordinate system (x, y) such that the velocity component u is parallel to the plate and is taken to be the x-axis while v is perpendicular to the plate and is taken to be in the y-axis. The flow is assumed to be parallel to the plate, that is, along the x-axis. The geometry of the problem is given in Figure 1.

The system of equations for the flow of a nanofluid with thermophoresis and a binary chemical reaction with Arrhenius activation energy can be written as follows.

$$\frac{\partial v}{\partial y} = 0, \tag{1}$$

$$\frac{\partial u}{\partial t} + v\frac{\partial u}{\partial y} = \frac{\mu}{\rho f_\infty}\frac{\partial^2 u}{\partial y^2} + (1 - C_\infty)\, g\beta\rho f_\infty\, (T - T_\infty) - (\rho_p - \rho f_\infty)\, g(C - C_\infty), \tag{2}$$

$$\frac{\partial T}{\partial t} + v\frac{\partial T}{\partial y} = \alpha\frac{\partial^2 T}{\partial y^2} + \frac{\mu}{(\rho c_p)_f}\left(\frac{\partial u}{\partial y}\right)^2 + \tau\left\{ D_B\frac{\partial T}{\partial y}\,\frac{\partial C}{\partial y} + \frac{D_T}{T_\infty}\left(\frac{\partial T}{\partial y}\right)^2 \right\}, \tag{3}$$

$$\frac{\partial C}{\partial t} + v\frac{\partial C}{\partial y} = D_B\frac{\partial^2 C}{\partial y^2} - k_r^2\left(\frac{T}{T_\infty}\right)^n \text{Exp}\left(-\frac{E_a}{kT}\right)(C - C_\infty) + \frac{D_T}{T_\infty}\frac{\partial^2 T}{\partial y^2}. \tag{4}$$

5

$$\alpha = \frac{k_m}{(\rho c)_f} \quad \text{and} \quad \tau = \frac{(\rho c)_p}{(\rho c)_f}$$

The boundary conditions for equations (1)-(4) are given in the form:

$$u = U_0, \quad -k_f \frac{\partial T}{\partial y} = h_f(T_f - T), \quad D_B \frac{\partial C}{\partial y} + \frac{D_T}{T_\infty} \frac{\partial T}{\partial y} = 0, \quad \text{at} \quad y = 0, \quad t > 0$$
$$u \to 0, \quad T \to T_\infty, \quad C \to C_\infty \quad \text{as} \quad y \to \infty, \quad t > 0 \tag{5}$$

where (u, v) are the velocity components along (x, y) directions, respectively, μ is the viscosity, ρf_∞ is the density of the base fluid, g is the acceleration due to gravity, β is the volumetric thermal expansion coefficient of the nanofluid, ρ_p is the density of nanoparticle, T is the temperature, C is the concentration of the fluid, α is the thermal diffusivity of the base fluid, c_p is the specific heat at constant pressure, τ is the ratio of the effective heat capacity of the nanoparticle material and heat capacity of the fluid, D_B is the Brownian diffusion coefficient, D_T is the thermophoretic diffusion coefficient, k_m is the thermal conductivity, $(\rho c)_f$ is the heat capacity of the base fluid and $(\rho c)_p$ is the effective heat capacity of the nanoparticle material, k_r^2 is the chemical reaction rate constant, $(T/T_\infty)^n \texttt{Exp}(-E_a/kT)(C - C_\infty)$ is Arrhenius function, n is a constant exponent and E_a is the Activation energy.

3. Transformation of equations

The velocity components are given by [17, 18]

$$u = U_0 f(\eta) \quad \text{and} \quad v = -\frac{v_0 \nu}{\delta(t)}, \tag{6}$$

where η is the similarity variable $\left(\eta = \frac{y}{\delta(t)}\right)$, $\delta(t)$ is a scaling parameter, f represents the scaled velocity and v_0 is the suction/injection velocity.

The temperature and concentrations are represented as

$$T = T_\infty + (T_f - T_\infty)\theta(\eta) \quad \text{and} \quad C = C_\infty + (C_w - C_\infty)\phi(\eta) \tag{7}$$

$\theta(\eta)$ is the dimensionless temperature and $\phi(\eta))$ is the dimensionless concentration. On using

6

Eqs. (6) and (7), Eqs. (2)-(4) transform into the following boundary value problem

$$f'' + (A\eta + v_0) f' + \frac{Gr}{Re} (\theta - Nr\phi) = 0, \tag{8}$$

$$\theta'' + Pr (A\eta + v_0) \theta' + PrEcf'^2 + PrNb\theta'\phi' + PrNt\theta'^2 = 0, \tag{9}$$

$$\phi'' + Sc (A\eta + v_0) \phi' - Sc\lambda^2 (1 + n\gamma\theta) \text{Exp} \left(-\frac{E}{1 + \gamma\theta} \right) \phi + \frac{Nt}{Nb}\theta'' = 0, \tag{10}$$

$$f (0) = 1, \quad f (\infty) \to 0, \tag{11}$$

$$\theta' (0) = -Bi(1 - \theta(0)), \quad \theta (\infty) \to 0, \tag{12}$$

$$Nb\phi' + Nt\theta' (0) = 0, \quad \phi (\infty) \to 0. \tag{13}$$

The prime denotes differentiation with respect to η. The parameters in equations (8)-(13) are the unsteadiness parameter A, scaling parameter δ, Grashof number Gr whic is the ratio of the buoyancy to viscous force acting on a fluid, Reynolds number Re which is the ratio of inertial forces to viscous forces, Buoyancy ratio parameter Nr which is an upward force exerted on an object that is immersed in a fluid, Prandtl Pr, a ratio of momentum diffusivity to thermal diffusivity, Eckert number Ec which is ratio of advective transport to heat dissipation potential, Brownian motion parameter Nb the random movement of particles in a fluid, thermophoresis parameter Nt which is the movement of microscopic particles due to a force of a temperature gradient, Schmidt number Sc, a ratio of momentum diffusivity and mass diffusivity, the dimensionless chemical reaction rate constant λ^2, the temperature relative parameter γ, the dimensionless activation energy E and Biot number Bi which is the ratio of the heat transfer resistances inside of and at the surface of a body. These parameters are defined as;

$$A = \frac{\delta\delta'}{\nu}, \quad \delta(t) = \sqrt{2A\nu t + L^2}, \quad Gr = \frac{(1 - C_\infty) g\beta\rho f_\infty \triangle T \ \delta^3}{\nu^2}, \quad Re = \frac{U_0\delta}{\nu},$$

$$Nr = \frac{(\rho_p - \rho f_\infty) \triangle C}{(1 - C_\infty)\rho f_\infty \beta\Delta T}, \quad Pr = \frac{\nu}{\alpha}, \quad Ec = \frac{U_0^2}{c_p (T_f - T_\infty)}, \quad Nb = \frac{\tau D_B \triangle C}{\nu},$$

$$Nt = \frac{\tau D_T \triangle T}{\nu T_\infty}, \quad Sc = \frac{\nu}{D_B}, \quad \lambda^2 = \frac{k_r^2\delta^2}{\nu}, \quad \gamma = \frac{T_f - T_\infty}{T_\infty}, \quad E = \frac{E_a}{kT_\infty}, \quad Bi = \frac{h_f}{k_f}\delta(t).$$

7

4. Heat and mass transfer coefficients

The heat transfer rate from the surface of the plate is given by

$$q_w = -k \left[\frac{\partial T}{\partial y} \right]_{y=0},$$ (14)

The local Nusselt number is defined as

$$Nu = \frac{\delta q_w}{k \left(T_f - T_\infty \right)}.$$ (15)

$$Nu = -\theta'(0).$$ (16)

The mass flux at the surface of the wall is given by

$$q_m = -D_m \left[\frac{\partial C}{\partial y} \right]_{y=0}$$ (17)

The local Sherwood is defined as

$$Sh = \frac{\delta q_m}{D_m (C_w - C_\infty)}.$$ (18)

Using Eq. (17) in Eq. (18) the dimensionless Sherwood number obtained as

$$Sh = -\phi'(0).$$ (19)

5. Numerical Solution using Spectral Quasi-linearization Method

The set of ordinary differential eqs. (8)-(10) together with the boundary conditions (11)-(13) are solved using spectral quasi-linearization method to get a high accuracy. The fundamental principle of spectral collocation methods is that, given discrete data on a grid, interpolate the data globally and, then evaluate the derivatives of the interpolant on the grid (Trefethen [21] and Canuto *et al.* [22]). The quasi-linearization method (QLM) is a generalization of the Newton-Raphson method (Bellman and Kalaba [23]). The derivation of the QLM is based on the linearization of the nonlinear components of the governing equations using

8

the Taylor series assuming that the difference between successive iterations, that is at $r+1$, and r is negligibly small. We solve the nonlinear system of ordinary differential equations with boundary conditions (11)-(13) using the spectral quasi-linearisation method (SQLM). The nonlinear components of the system of ordinary differential equations give the following iterative sequences of linear differential equations. First define functions F, Θ and Φ for the equations (8)-(10) respectively as;

$$F = f'' + (A\eta + v_0)f' + \frac{Gr}{Re}(\theta - Nr\phi), \tag{20}$$

$$\Theta = \theta'' + Pr(A\eta + v_0)\theta' + PrEcf'^2 + PrNb\theta'\phi' + PrNt\theta'^2, \tag{21}$$

$$\Phi = \phi'' + Sc(A\eta + v_0)\phi' - Sc\lambda^2(1 + n\gamma\theta)\text{Exp}\left(-\frac{E}{1 + \gamma\theta}\right)\phi + \frac{Nt}{Nb}\theta''. \tag{22}$$

We construct the errors from the iterative process for the the equations (8)-(10) as given by (23)-(25) respectively

$$a_{0r}f''_{r+1} + a_{1r}f'_{r+1} + a_{2r}\theta_{r+1} + a_{3r}\phi_{r+1} - F = R_f, \tag{23}$$

$$b_{0r}\theta''_{r+1} + a_{1r}\theta'_{r+1} + b_{2r}f'_{r+1} + b_{3r}\phi'_{r+1} - \Theta = R_\theta, \tag{24}$$

$$c_{0r}\phi''_{r+1} + c_{1r}\phi'_{r+1} + c_{2r}\phi_{r+1} + c_{3r}\theta''_{r+1} + c_{4r}\theta_{r+1} - \Phi = R_\phi. \tag{25}$$

subject to the boundary conditions

$$f_{r+1}(0) = 1, \quad f_{r+1}(\infty) \to 0 \tag{26}$$

$$\theta'_{r+1}(0) = -Bi(1 - \theta(0)), \quad \theta_{r+1}(\infty) \to 0 \tag{27}$$

$$Nb\phi'_{r+1}(0) + Nt\theta'_{r+1}(0) = 0, \quad \phi_{r+1}(\infty) \to 0 \tag{28}$$

9

where the coefficients in (23)-(25) are given as;

$$
\begin{aligned}
& a_{0,r} = 1, \quad a_{1,r} = (A\eta + v_0), \quad a_{2,r} = \frac{Gr}{Re}, \quad a_{3,r} = -\frac{GrNr}{Re}, \quad b_{0,r} = 1, \\
& b_{1,r} = Pr(A\eta + v_0) + PrNb\phi_r' + 2PrNt\theta_r', b_{2,r} = 2PrEcf_r', \quad b_{3,r} = PrNb\theta_r', \\
& c_{0,r} = 1, \quad c_{1,r} = Sc(A\eta + v_0), \quad c_{2,r} = -Sc\lambda^2(1 + n\gamma\theta_r)e^{-E/(1+\gamma\theta_r)}, \quad c_{3,r} = \frac{Nt}{Nb} \\
& c_{4,r} = -\frac{Sc\lambda^2 e^{-E/(1+\gamma\theta_r)}(E + n + n(2 + E)\gamma\theta_r + n\gamma^2\theta_r^2)}{(1 + \gamma\theta_r)^2}
\end{aligned}
\tag{29}
$$

The initial guesses are selected as functions that satisfy the boundary conditions, and these were chosen as

$$
f_0(\eta) = e^{-\eta}, \quad \theta_0(\eta) = \frac{Bi}{1 + Bi}e^{-\eta}, \quad \phi_0(\eta) = -\frac{Nt}{Nb}\frac{Bi}{(1 + Bi)}e^{-\eta}. \tag{30}
$$

In order to apply the SQLM to solve the system of nonlinear ordinary differential (23)-(25) we transform the domain from $0 \le \eta \le L_x$ to $-1 \le x \le 1$ using the transformation $\eta = L_x(x + 1)/2$ [24]. We use the Gauss-Lobatto collocation points defined by

$$
x_i = \cos\left(\frac{\pi i}{N}\right), \quad i = 0, 1, 2, \cdots, N \tag{31}
$$

The spectral collocation method uses a differentiation matrix (D) to approximate the derivative of unknown variables at the collocation points as a matrix vector product. The D-matrix is constructed for the domain $[-1, 1]$ so we scale this matrix for the domain $[0, L_x]$ by taking $D1 = 2D/L_x$, so that

$$
\frac{dF_r^{(1)}}{d\eta}(\eta_j) = \sum_{k=0}^{n} D1f(\eta_k) = D1F_m, \quad j = 0, 1, 2, \cdots, N \tag{32}
$$

where $F = [f(\eta_0), f(\eta_1), f(\eta_2), \cdots, f(\eta_N)]^T$ represent the vector function at the collocation points. Higher order derivatives are given as powers of the scaled differentiation matrix

$$
F^{(p)} = D1^p F_r. \tag{33}
$$

10

Using the scaled differentiation matrix on (23)-(25) we obtain;

$$A_{11}f_{r+1} + A_{12}\theta_{r+1} + A_{13}\phi_{r+1} = R_f$$
$$A_{21}f_{r+1} + A_{22}\theta_{r+1} + A_{23}\phi_{r+1} = R_\theta \qquad (34)$$
$$A_{31}f_{r+1} + A_{32}\theta_{r+1} + A_{33}\phi_{r+1} = R_\phi$$

In matrix for this can be written as

$$
\begin{bmatrix} A_{11} & A_{12} & A_{13} \\ A_{21} & A_{22} & A_{23} \\ A_{31} & A_{32} & A_{33} \end{bmatrix}
\begin{bmatrix} f_{r+1} \\ \theta_{r+1} \\ \phi_{r+1} \end{bmatrix}
=
\begin{bmatrix} R_f \\ R_\theta \\ R_\phi \end{bmatrix}
$$

where

$A11 = diag(a_{0,r})D2 + diag(a_{1,r})D1, \ A12 = diag(a_{2,r})I, \ A13 = diag(a_{3,r})I$

$A21 = diag(b_{2,r})D1, \ A22 = diag(b_{0,r})D2 + diag(b_{1,r})D1, \ A23 = diag(b_{3,r})D1$

$A31 = Zeros(N+1, N+1), \ A32 = diag(c_{3,r})D2 + diag(c_{4,r})I,$

$A33 = diag(c_{0,r})D2 + diag(c_{1,r})D1 + diag(c_{2,r})I$

Residual error analysis

We validate the accuracy and convergence of the SQLM by performing a residual error analysis. We tabulate the residual errors in Table 1 and Figure 2.

11

Table 1: Residual error for different iterations

i	$f(\eta)$	$\theta(\eta)$	$\phi(\eta)$
1	7.867129×10^{-11}	3.191528×10^{-1}	2.535005×10^{-1}
2	3.159872×10^{-11}	7.612455×10^{-4}	1.025387×10^{-3}
3	8.640200×10^{-11}	4.233677×10^{-9}	4.432544×10^{-7}
4	8.753887×10^{-11}	9.773146×10^{-11}	2.045453×10^{-11}
5	9.731593×10^{-11}	2.188154×10^{-10}	6.840795×10^{-11}
6	1.182343×10^{-10}	7.860722×10^{-10}	2.582401×10^{-11}
7	7.753442×10^{-11}	3.279255×10^{-10}	5.194600×10^{-11}
8	5.161382×10^{-11}	3.652539×10^{-10}	4.351142×10^{-11}
9	3.808154×10^{-11}	3.276447×10^{-10}	5.004180×10^{-11}
10	8.185452×10^{-11}	5.311367×10^{-10}	2.323225×10^{-11}

From Table 1 we note that the smallest values for residual errors were attained after 2 iterations for $f(\eta)$ and 4 iterations for $\theta(\eta)$ and $\phi(\eta)$. This shows that the SQLM is an accurate method awith a good convergence rate. In order to have clearer picture on the convergence rates we plot the residual errors against number of iterations in Figure 2.
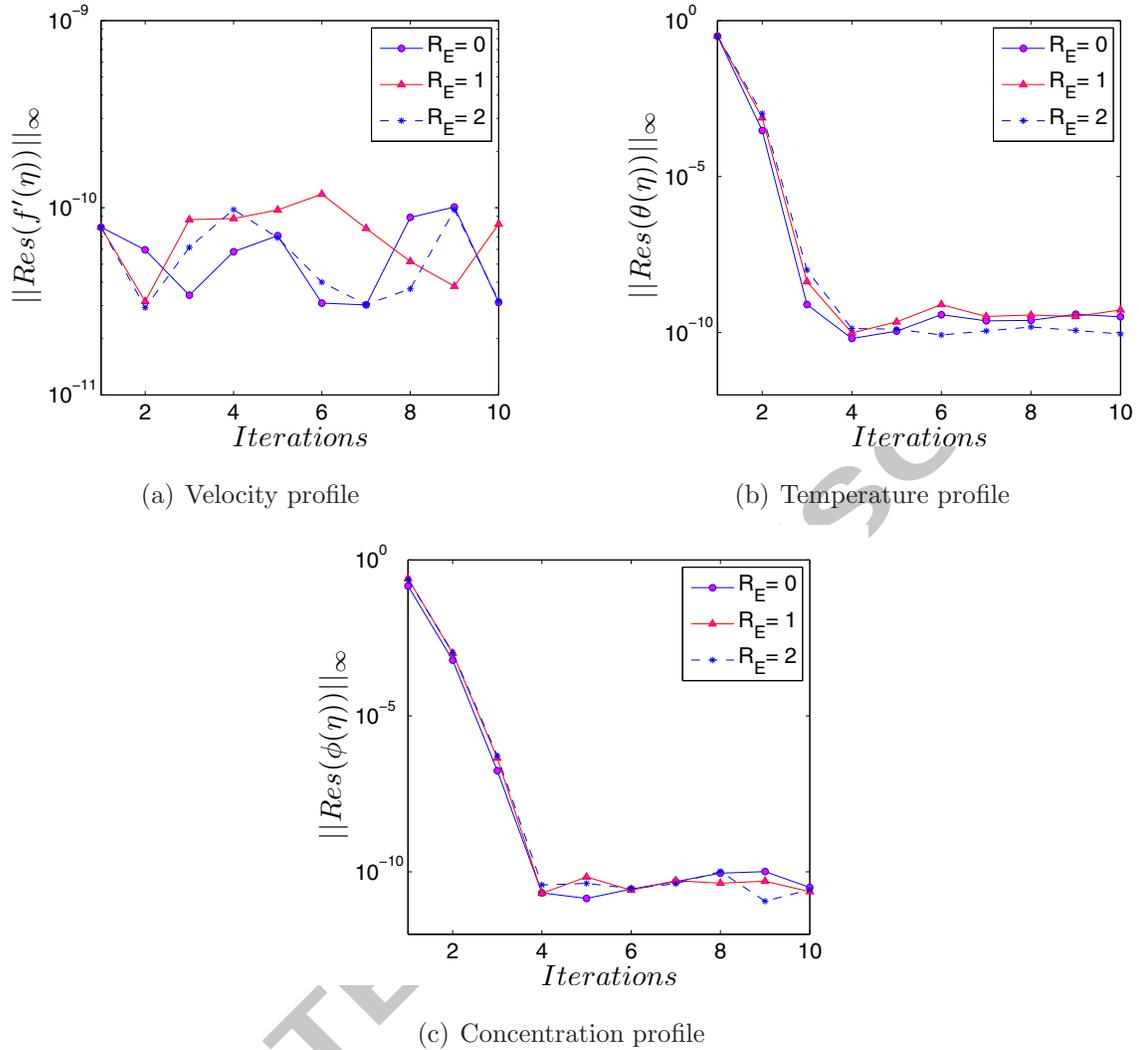
(a) Velocity profile

(b) Temperature profile

(c) Concentration profile

Figure 2: Residual errors for velocity, temperature and concentration profiles

6. Discussion of Results

In this paper we investigate the impact that the activation energy has on a binary chemical reacting nanofluid with convective boundary conditions. We investigate the influence that the thermal and chemical parameters have on the velocity, temperature and concentration of the fluid in the boundary layer. We begin by investigating how the drag, heat transfer and mass transfer on the solid boundary are affected by certain parameters. We do so by varying a parameter of interest while keeping the rest constant and note the changes to the

13

local skin friction coefficient (C_f), local Nusselt (Nu) number and local Sherwood number (Sh). The results are given in Table 2.

Table 2: Effect of varying parameters on skin friction coefficient (C_f), local Nusselt number (Nu) and local Sherwood number (Sh) and $v_0 = 2$, $Gr = 1.5$, $Re = 1$, $Bi = 100$, $Ec = 0.2$, $\gamma = 1$, $n = 1$, $Pr = 6.8$
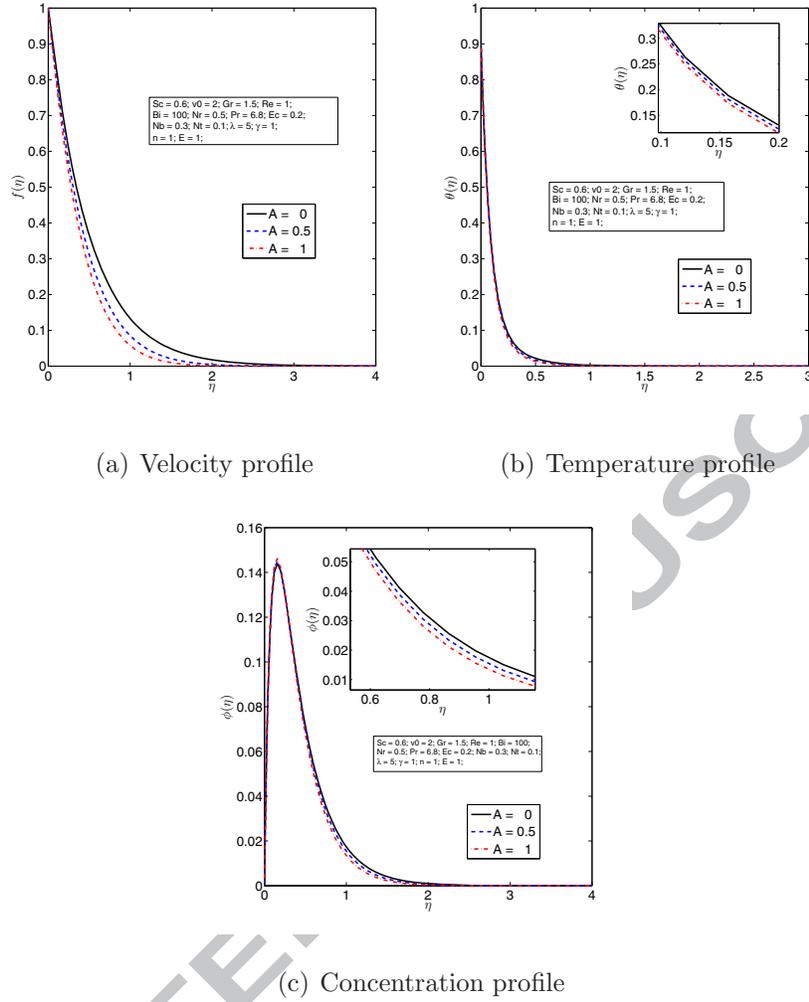
A	Sc	Nr	Nb	Nt	E	λ	$-f'(0)$	$-\theta'(0)$	$-\phi'(0)$
0.0	0.6	0.5	0.3	0.1	1.0	5.0	1.912449	9.865404	-2.739898
0.5	0.6	0.5	0.3	0.1	1.0	5.0	2.126137	9.941617	-2.759319
1.0	0.6	0.5	0.3	0.1	1.0	5.0	2.293911	10.037429	-2.785280
1.0	0.3	0.5	0.3	0.1	1.0	5.0	2.322190	10.238323	-2.987516
1.0	0.0	0.5	0.3	0.1	1.0	5.0	2.789233	10.291383	-3.400554
1.0	0.6	0.25	0.3	0.1	1.0	5.0	2.269238	10.052712	-2.790421
1.0	0.6	0.0	0.3	0.1	1.0	5.0	2.244563	10.067812	-2.795502
1.0	0.6	0.5	0.2	0.1	1.0	5.0	2.318582	10.021971	-4.170131
1.0	0.6	0.5	0.1	0.1	1.0	5.0	2.392579	9.974499	-8.292432
1.0	0.6	0.5	0.3	0.2	1.0	5.0	2.332045	9.108249	-4.947295
1.0	0.6	0.5	0.3	0.3	1.0	5.0	2.367588	8.191294	-6.501718
1.0	0.6	0.5	0.3	0.1	0.5	5.0	2.283544	9.900079	-2.607755
1.0	0.6	0.5	0.3	0.1	0.0	5.0	2.274071	9.751707	-2.413290
1.0	0.6	0.5	0.3	0.1	1.0	2.5	2.322548	10.342466	-3.182157
1.0	0.6	0.5	0.3	0.1	1.0	0.0	2.346528	10.524261	-3.413481

In Table 3 we give a summary of the parameter values in the model and the sources from which they were obtained.

14
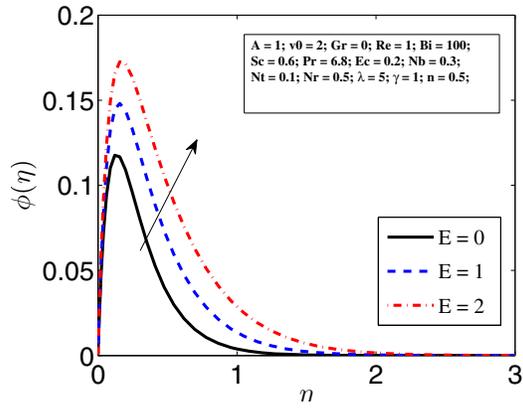
Table 3: Parameters in the model and their values

Parameter	Symbol	Value	Source
Grashof number	Gr	(0.1, 5)	[1]
Reynolds number	Re	1	assumed
Buoyancy parameter	Nr	(0.3, 1.2)	[25]
Prandtl number	Pr	(6.8, 7.2)	[16]
Eckert number	Ec	(0.1, 0.4)	[26]
Brownian motion parameter	Nb	0.5	[27]
Thermophoresis parameter	Nt	0.5	[27]
Schmidt number	Sc	0.6	[1, 17]
Chemical reaction constant	λ^2	5	[1, 17, 18]
temperature relative parameter	γ	(0, 5)	[20]
Activation energy	E	1	[1, 17, 20]
Biot number	Bi	(0.1, 100)	[28, 29, 30]
suction/injection parameter	v_0	(-3, 3)	[1, 17]
Steadiness parameter	A	(0, 1)	[17]
Constant exponent	n	(-1, 1)	[17, 20]

The unsteady parameter A is investigated in Figure 3 by plotting the velocity, temperature and concentration profiles for different values of the parameter. Increasing the unsteady parameter from the steady value of 0, led to a decrease in the velocity, temperature and concentration in the boundary layer. As the fluid transition from laminar flow to turbulent flow the velocity, heat transfer and mass transfer all decrease. Results from the current study are consistent with results from [17]. The overshoot in the concentration profile can be attributed other factors not the unsteady parameter. The effect of the unsteady parameter is analyzed by comparing the curves for different values of the unsteady parameter.
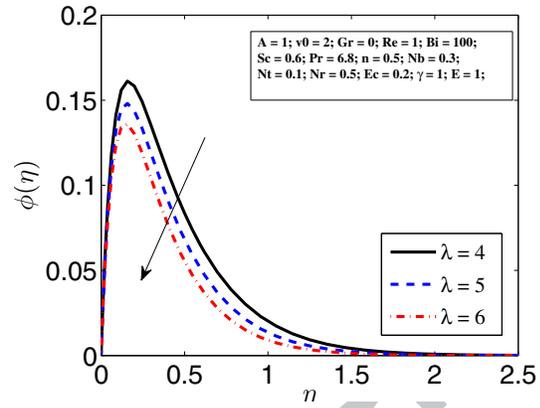
15

(a) Velocity profile

(b) Temperature profile

(c) Concentration profile

Figure 3: Effect of unsteady parameter A

We note that the velocity and temperature are not affected by most parameters and as such we turn our focus to parameters that are associated with the activation energy and chemical reaction. The graph for effect of different parameters on the concentration profiles are given in Figure 4. An increase in the activation energy parameter E and the thermophoretic parameter Nt leads to an increase in the chemical species concentration at the boundary layer. The observation on the thermophoretic parameter is not consistent with the expected outcomes. Thermophoresis leads to a net movement of particles from a hotter region to a colder region. This has applications in removing small particles from gas streams and determining
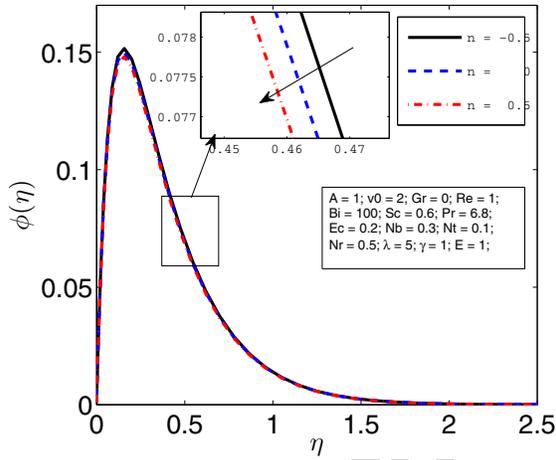
16

exhaust gas projectiles. Results from [31] showed that the concentration of the nanoparticles was higher on the cold wall(nanopartcle accumulation) and lower near the adiabatic wall(nanoparticle depletion). Similar results were obtained by Malvandi ans Ganji [32] who showed that the concentration of nanoparticles in the core of the microchannel was higher than near the heated wall. In this study the results are contrary to the expected results, that is, the concentration is seen to increase with increasing values of thermophoretic parameter in the boundary layer. This observation can be attributed to the confounding effect of the thermophoretic parameter and activation energy. An increase in the thermophoretic parameter is associated with an increase in temperature Figure 5, which is also associated with an increase in activation energy thereby increasing the rate of chemical reaction leading to a high concentration in the boundary layer. Similar results can be found in [33]. However increasing the constant exponent n, Brownian motion parameter Nb and the chemical reaction constant λ causes a decrease in the chemical species within the boundary layer. These results are consistent with the expected results. The Brownian motion parameter increases the 'indecisive' random movement of molecules. Increasing the Brownian motion increases the the movement of molecules in and out of the boundary layer and the free stream. Since the free stream is relatively large compared to the boundary layer some of the molecules that enter the free stream may not 'come back' into the boundary layer resulting in a net decrease in concentration of molecules in the boundary layer. Similar results for Brownian were drawn by Mustafa *et al.* [34] and Mabood *et al.* [33].
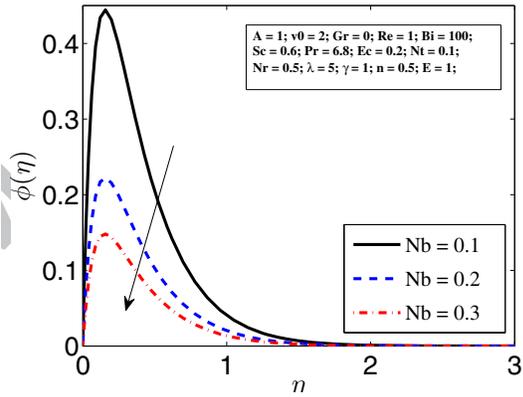
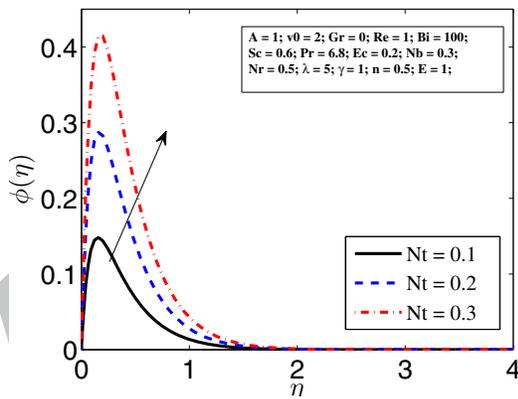(a) Profile for Activation energy
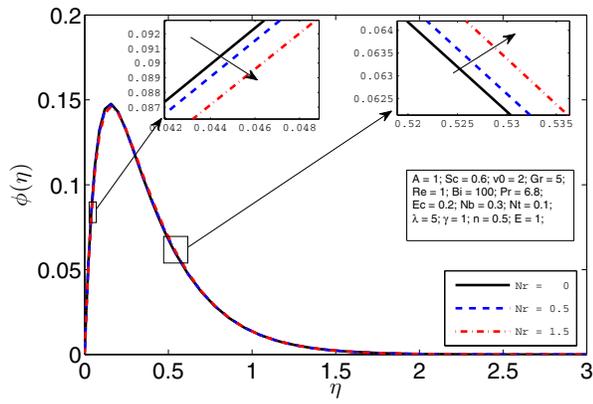
(b) Profile chemical reaction constant

(c) Profile for unit less constant exponent

(d) Profile for Brownian motion parameter

(e) Profile for thermophoretic parameter

(f) Profile for buoyancy parameter

Figure 4: Concentration profiles for different parameters

The viscous dissipation is analyzed by making obsrvations of changes in the temperature profile for varying values of the Eckert number Ec in Figure 5. Increasing the Eckert number increases the temperature of the fluid leading to thickening of the thermal boundary layer which is consistent with heat generation due to the frictional effects of the fluid. These observations are consistent with those found in literature such as [35, 36]. We also observe the positive correlation between the temperature and the thermophoretic force. Increasing the temperature of the fluid will result in an increase in the thermophoretic parameter.

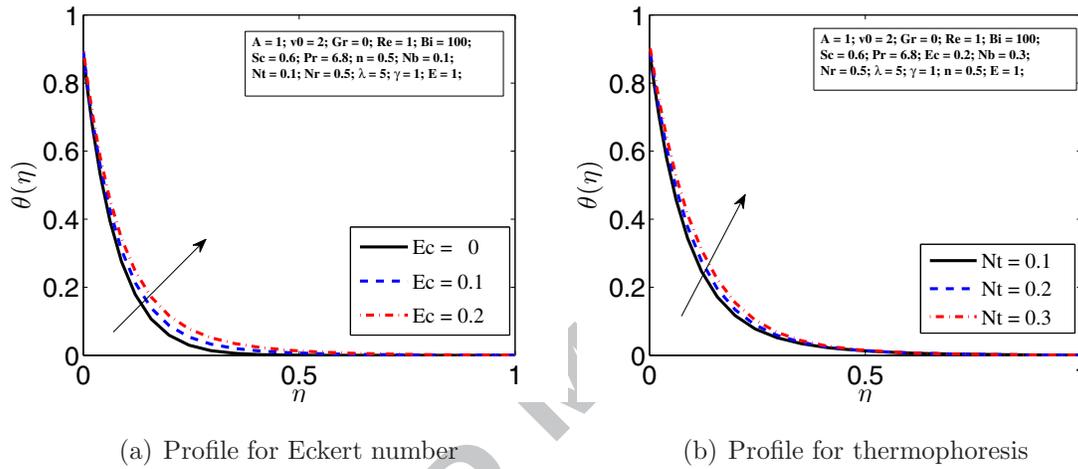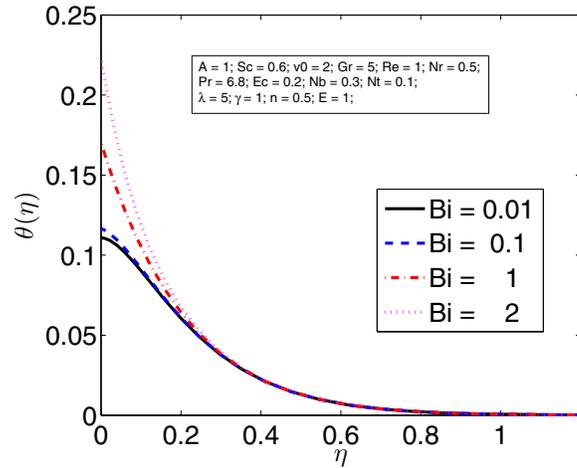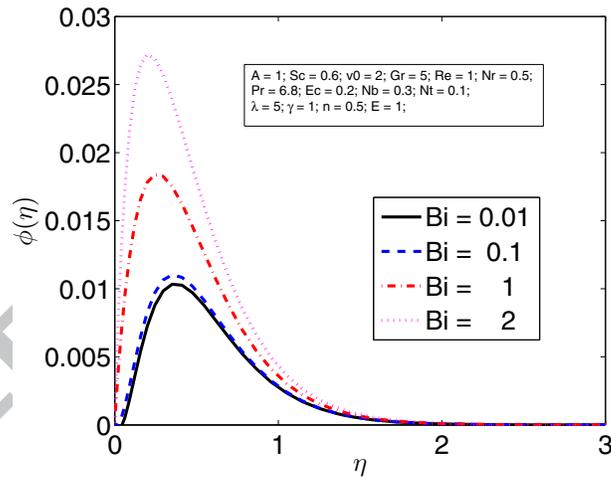(a) Profile for Eckert number

(b) Profile for thermophoresis

Figure 5: Temperature profile for the Eckert number and thermophoresis

We analyze the effect of Biot number on the temperature and concentration in Figure 6. It is shown that increasing the Biot number will result in a increase in both the temperature and concentration in the boundary layer. Since we considered a plate of infinite length, this means the length scale is long enough so that the the Biot number exceed one. This implies that heat resistance offered at the surface is less than heat resistance offered within the solid plate. Temperature gradients within the solid are no longer negligible, we can no longer assume constant temperature within the solid. This is so since the plate is heated to maintain a constant temperature yet it is constantly being cooled at the surface by the fluid it comes in contact with. The transfer of thermal energy from the solid to the fluid results in an increase in the thermal energy of the fluid leading to an increase in the fluid temperature and concentration of the chemical species as a result of an increase in the chemical reaction.

19

The result on the effect of Biot number on concentration in this study concurs with result by Makinde and Aziz [37]. They showed that concentration increased for increasing values of the Biot number.

A = 1; Sc = 0.6; v0 = 2; Gr = 5; Re = 1; Nr = 0.5;
Pr = 6.8; Ec = 0.2; Nb = 0.3; Nt = 0.1;
$\lambda = 5; \gamma = 1; n = 0.5; E = 1;$

(a) Temperature profile

A = 1; Sc = 0.6; v0 = 2; Gr = 5; Re = 1; Nr = 0.5;
Pr = 6.8; Ec = 0.2; Nb = 0.3; Nt = 0.1;
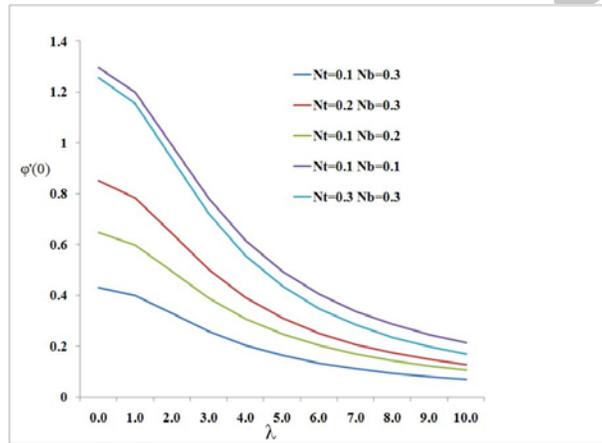$\lambda = 5; \gamma = 1; n = 0.5; E = 1;$

(b) Concentration profile

Figure 6: An analysis of the influence of Biot number on temperature and concentration profiles

Figure 7 seeks to give an analysis of the chemical reaction constant λ by taking values from 0 to 1 in the step of 0.1. It is shown that the chemical reaction constant causes the concentration to decrease in a nonlinear pattern in the boundary layer. Pal and Mondal [38]

20

also drew similar conclusion for this parameter. The analysis is done for different values of Brownian motion Nb and thermophoresis Nt by fixing values for one parameter and varying the other parameter in three steps (0.1, 0.2 and 0.3). The least concentration occurs when both Nb and Nt have values of 0.3 and is highest when both parameters have values of 0.1. For fixed values of Nb (0.3) and varying Nt the concentration increases with increasing values of Nt and this is consistent with observation made earlier on the influence of thermophoresis on concentartion. The concentration showed a decreasing trend for increasing values of Nb and fixed values of Nt (0.1). This too is is consistent with earlier observation made for effect of Brownian motion on concentration.

(a) Concentration profile for chemical reaction rate constant λ

Figure 7: Analysis of the effect of chemical reaction parameter (λ) on the concentration for different values of Nb and Nt

Figure 8 seek to give an analysis of the effect of varying the Eckert number on the temperature for different values of the Brownian motion parameter and thermophoresis parameter. Increasing the thermophoresis parameter increases the temperature while the Brownian motion has no effect on the temperature. This observation is consistent with the previous observation that we made, the thermophoretic force is in the direction of a lower temperature and this will result in temperature increase in that region and Brownian motion is by a random process that has no bearing on the temperature difference of any two regions and
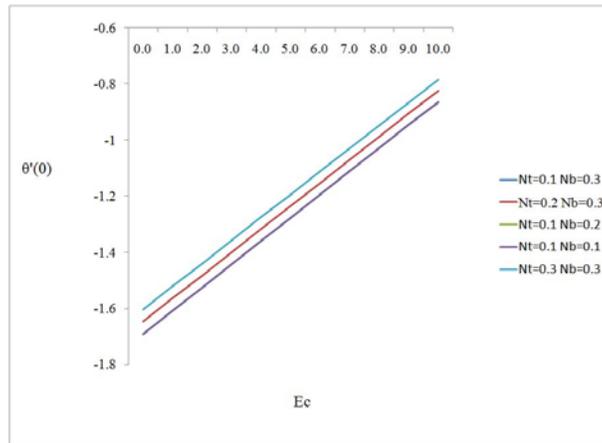
21

thus it does not affect the temperature.

Figure 8: Temperature profile for the Eckert number with varying Nt and Nb

7. Conclusion

In this paper we considered the effect of activation energy, Brownian motion and thermophoresis on a binary chemical unsteady nanofluid with convective boundary conditions. The governing nonlinear partial differential equations are reduced to second order nonlinear ordinary differential equations using an appropriate similarity transformation and solved using the spectral quasi-linearization method. The following observations were made.

- The unsteady parameter reduces the velocity and temperature of the fluid while on the other hand increases the concentration of the chemical species in the boundary layer,

- The activation energy and thermophoresis parameters increase the concentration of the chemical species in the boundary layer while the Brownian motion and the chemical reaction constant reduces the concentration of the chemical species in the same region.

- The Eckert and the thermophoresis parameters are found to increase the temperature of the fluid.

22

Acknowledgment

[1] O. D. Makinde and P. O. Olanrewaju. Unsteady mixed convection with soret and dufour effects past a porous plate moving through a binary mixture of chemically reacting fluid. *Chemical Engineering Communications*, 198(7):920–938, 2011.

[2] Z. Shafique, M. Mustafa, and A. Mushtaq. Boundary layer flow of maxwell fluid in rotating frame with binary chemical reaction and activation energy. *Results in physics*, 6:627–633, 2016.

[3] F. Lazaridis, A. Savara, and P. Argyrakis. Reaction efficiency effects on binary chemical reactions. *The Journal of chemical physics*, 141(10):104103, 2014.

[4] H. Pedersen and S. D. Elliott. Studying chemical vapor deposition processes with theoretical chemistry. *Theoretical Chemistry Accounts*, 133(5):1476, 2014.

[5] T. Rana, M. V. S. Chandrashekhar, and T. S. Sudarshan. Elimination of silicon gas phase nucleation using tetrafluorosilane (sif4) precursor for high quality thick silicon carbide (sic) homoepitaxy. *physica status solidi (a)*, 209(12):2455–2462, 2012.

[6] H. B. Profijt, S. E. Potts, M. C. M. Van de Sanden, and W. M. M. Kessels. Plasma-assisted atomic layer deposition: basics, opportunities, and challenges. *Journal of Vacuum Science & Technology A: Vacuum, Surfaces, and Films*, 29(5):050801, 2011.

[7] J. Sun and Y. C. Sun. Chemical liquid phase deposition of thin aluminum oxide films. *Chinese Journal of Chemistry*, 22(7):661–667, 2004.

[8] S. U. S. Choi and J. A. Eastman. Enhancing thermal conductivity of fluids with nanoparticles. Technical report, Argonne National Lab., IL (United States), 1995.

[9] K. Das, R. P. Sharma, and A. Sarkar. Heat and mass transfer of a second grade magnetohydrodynamic fluid over a convectively heated stretching sheet. *Journal of Computational Design and Engineering*, 3(4):330–336, 2016.

[10] S. Nadeem, S. Ahmad, and N. Muhammad. Computational study of falkner-skan problem for a static and moving wedge. *Sensors and Actuators B: Chemical*, 263:69–76, 2018.

[11] N. Muhammad, S. Nadeem, and M. T. Mustafa. Analysis of ferrite nanoparticles in the flow of ferromagnetic nanofluid. *PloS one*, 13(1):e0188460, 2018.

[12] N. Muhammad and S. Nadeem. Ferrite nanoparticles ni-znfe2o4, mn-znfe2o4 and fe2o4 in the flow of ferromagnetic nanofluid. *The European Physical Journal Plus*, 132(9):377, 2017.

[13] N. Muhammad, S. Nadeem, and R. U. l. Haq. Heat transport phenomenon in the ferromagnetic fluid over a stretching sheet with thermal stratification. *Results in physics*, 7:854–861, 2017.

[14] Y. S. Daniel, Z. A. Aziz, Z. Ismail, and F. Salah. Thermal stratification effects on mhd radiative flow of nanofluid over nonlinear stretching sheet with variable thickness. *Journal of Computational Design and Engineering*, 5(2):232–242, 2017.

[15] O. D. Makinde, P. Olanrewaju, and W. M. Charles. Unsteady convection with chemical reaction and radiative heat transfer past a flat porous plate moving through a binary mixture. *Afrika Matematika*, 22(1):65–78, 2011.

[16] Z. Abbas, M. Sheikh, and S. S. Motsa. Numerical solution of binary chemical reaction on stagnation point flow of casson fluid over a stretching/shrinking sheet with thermal radiation. *Energy*, 95:12–20, 2016.

[17] Kh. A. Maleque. Effects of exothermic/endothermic chemical reactions with arrhenius activation energy on mhd free convection and mass transfer flow in presence of thermal radiation. *Journal of Thermodynamics*, Article ID 692516:11, 2013.

[18] Kh. A Maleque. Effects of binary chemical reaction and activation energy on mhd boundary layer heat and mass transfer flow with viscous dissipation and heat generation/absorption. *ISRN Thermodynamics*, Article ID 284637:9, 2013.

[19] S. Nadeem, S. Ahmad, N. Muhammad, and M. T. Mustafa. Chemically reactive species in the flow of a maxwell fluid. *Results in physics*, 7:2607–2613, 2017.

[20] F. G. Awad, S. Motsa, and M. Khumalo. Heat and mass transfer in unsteady rotating fluid flow with binary chemical reaction and activation energy. *PloS one*, 9(9):e107622, 2014.

[21] L. N. Trefethen. *Spectral methods in MATLAB*, volume 10. Siam, 2000.

[22] C Canuto, M Y Hussaini, Al Quarteroni, A Thomas Jr, et al. *Spectral methods in fluid dynamics*. Springer Science & Business Media, 2012.

[23] R. E. Bellman and R. E. Kalaba. Quasilinearization and nonlinear boundary-value problems. 1965.

[24] P. K. Kameswaran, P. Sibanda, and S. S. Motsa. A spectral relaxation method for thermal dispersion and radiation effects in a nanofluid flow. *Boundary Value Problems*, 2013(1):242, 2013.

[25] D. Pal and H. Mondal. The influence of thermal radiation on hydromagnetic darcy-forchheimer mixed convection flow past a stretching sheet embedded in a porous medium. *Meccanica*, 46(4):739–753, 2011.

[26] G. Makanda, O. D. Makinde, and P. Sibanda. Natural convection of viscoelastic fluid from a cone embedded in a porous medium with viscous dissipation. *Mathematical Problems in Engineering*, Article ID 934712:11, 2013.

[27] H. Sithole, H. Mondal, and P. Sibanda. Entropy generation in a second grade magneto-hydrodynamic nanofluid flow over a convectively heated stretching sheet with nonlinear thermal radiation and viscous dissipation. *Results in Physics*, 9:1077–1085, 2018.

[28] M. d. Uddin, W. A. Khan, A. I. Ismail, et al. Scaling group transformation for mhd boundary layer slip flow of a nanofluid over a convectively heated stretching sheet with heat generation. *Mathematical problems in Engineering*, Article ID 934964:20, 2012.

[29] C. h. RamReddy, P. V. S. N. Murthy, A. J. Chamkha, and A. M. Rashad. Soret effect on mixed convection flow in a nanofluid under convective boundary condition. *International Journal of Heat and Mass Transfer*, 64:384–392, 2013.

[30] P. K. Kameswaran, P. Sibanda, and A. S. N. Murti. Nanofluid flow over a permeable surface with convective boundary conditions and radiative heat transfer. *Mathematical Problems in Engineering*, Article ID 201219:11, 2013.

[31] A. Malvandi and D. D. Ganji. Effects of nanoparticle migration on force convection of alumina/water nanofluid in a cooled parallel-plate channel. *Advanced Powder Technology*, 25(4):1369–1375, 2014.

[32] A. Malvandi and D. D. Ganji. Brownian motion and thermophoresis effects on slip flow of alumina/water nanofluid inside a circular microchannel in the presence of a magnetic field. *International Journal of Thermal Sciences*, 84:196–206, 2014.

[33] F. Mabood, W. A. Khan, and A. I. M. d. Ismail. Mhd boundary layer flow and heat transfer of nanofluids over a nonlinear stretching sheet: a numerical study. *Journal of Magnetism and Magnetic Materials*, 374:569–576, 2015.

[34] M. Mustafa, J. A. Khan, T. Hayat, and A. Alsaedi. Buoyancy effects on the mhd nanofluid flow past a vertical surface with chemical reaction and activation energy. *International Journal of Heat and Mass Transfer*, 108:1340–1346, 2017.

[35] M. H. Yazdi, S. Abdullah, I. Hashim, and K. Sopian. Effects of viscous dissipation on the slip mhd flow and heat transfer past a permeable surface with convective boundary conditions. *Energies*, 4(12):2273–2294, 2011.

[36] A. Mahdy and A. J. Chamkha. Chemical reaction and viscous dissipation effects on darcy-forchheimer mixed convection in a fluid saturated porous media. *International Journal of Numerical Methods for Heat & Fluid Flow*, 20(8):924–940, 2010.

[37] O. D. Makinde and A. Aziz. Boundary layer flow of a nanofluid past a stretching sheet with a convective boundary condition. *International Journal of Thermal Sciences*, 50(7):1326–1332, 2011.

[38] D. Pal and H. Mondal. Influence of chemical reaction and thermal radiation on mixed convection heat and mass transfer over a stretching sheet in darcian porous medium with soret and dufour effects. *Energy conversion and management*, 62:102–108, 2012.

Highlights:

- Combined effects of activation energy and binary chemical reaction are proposed.
- Spectral quasi-linearization method (SQLM) is used for computer simulations.
- Use Arrhenius activation energy in the chemical species concentration.
- Validate the accuracy and convergence using residual error analysis.